Åbo Akademi
University

Some Defects in Two-Dimensional Spin-$\frac{1}{2}$ Heisenberg Antiferromagnets: a Numerical Study of Magnetic Effects

Kaj Höglund

Physics
Department of Natural Sciences
Åbo Akademi University
Åbo 2010

Kaj Höglund
Some Defects in Two-Dimensional Spin-$\frac{1}{2}$ Heisenberg Antiferromagnets: a Numerical Study of Magnetic Effects
2010

Some Defects in Two-Dimensional Spin-$\frac{1}{2}$ Heisenberg Antiferromagnets: a Numerical Study of Magnetic Effects

Kaj Höglund

Physics
Department of Natural Sciences
Åbo Akademi University
Åbo 2010

Supervisor:

Prof. Anders Sandvik
Boston University

Pre-examiners:

Prof. Olav Syljuåsen
University of Oslo

Prof. Jussi Timonen
University of Jyväskylä

Opponent for the public defence:

Prof. Sebastian Eggert
University of Kaiserslautern

ISBN 978-952-12-2415-7
Uniprint – Åbo 2010

Acknowledgements

This thesis reports on work I participated in during 2000–2008. In the fall of that first year, Professor Anders Sandvik had returned to Åbo Akademi University, where he was setting up research within the field of computational condensed matter physics. He became my mentor and supervised this work, which turned out to take more time than he probably expected to start with, and what is usually considered normal. I am very thankful for his great patience in guiding me over the years, and feel fortunate to have been given the opportunity to participate in some truly exciting and relevant work. For showing me how to work and write scientifically, and for introducing me to so many nice people, I owe him a lot.

A generous part of our endeavors was inspired by the work of Professor Subir Sachdev and coworkers. Moreover, on many occasions throughout the work, the counsel of Prof. Sachdev played an important part in how events evolved, and it is regarded the highest.

A colleague once said, *physics is done on one's behind*. Mine had a sanctuary at ÅA's Physics Department. There, over the years, faculty and students provided an educating, enjoyable, and very fun place to work in. For this, each and every one is warmly acknowledged.

The computer simulations were performed on two dedicated Linux clusters. They were built and configured, maintained, and, eventually, dismantled by Dr. Kjell-Mikael Källman. For his efforts and helpfulness, throughout the years, he is sincerely acknowledged. Some of the computations were carried out at CSC – IT Center for Science.

Travel grants awarded by the Magnus Ehrnrooth Foundation, Stiftel-

sens för Åbo Akademi forskningsinstitut, and the Finnish Academy of Science from the Vilho, Yrjö, and Kalle Väisälä Foundation, have been very much appreciated.

March 21, 2010
Åbo

Contents

Outline of thesis

This thesis consists of a synopsis and five publications. Therefore, it has two parts. Part I outlines the topics covered in the publications, referred to as Papers 1–5, and also discusses some previously unpublished results. The publications are reproduced in Part II.

My thesis is devoted to the numerical study of the two-dimensional spin-$\frac{1}{2}$ Heisenberg antiferromagnet with defects. Namely, large-scale computer simulations were performed in order to determine how some defects, such as impurities and lattice boundaries, affect the magnetic properties of the Heisenberg host model. Part of the computational investigations were undertaken in order to test analytical predictions. Some of the background issues are touched upon in Chapter 1.

Chapter 2 deals with Papers 1 and 2. They report on the efforts I was involved in to determine the magnetic response of a single static spin-S impurity in a magnetically ordered Heisenberg system. In brief, a classical-like Curie prefactor—S^2 instead of $S(S+1)$—was numerically confirmed for the low-temperature impurity susceptibility, which, to some surprise, also turned out to have a previously overlooked contribution. A detailed narrative of those events can be found in my licentiate thesis [1], and, hence, the discussion is kept quite short in the present work. However, Paper 3 is a direct continuation of that work, albeit for a quantum critical Heisenberg model. In that case, our numerical data pointed towards a most curious behavior, as if the response of the impurity was that of a spin with irrational S, as, indeed, had been predicted by others on theoretical grounds. These events are summarized in Chapter 3. A

collaboration with the field-theoretical efforts of S. Sachdev resulted in Paper 4. Combining numerical data with analytical techniques, it deals with the spatial magnetic structure around said impurity at zero temperature. Mainly the numerical part of that story is covered in Chapter 4, which also presents results for the case of a magnetically ordered host model. Paper 5 pays attention to the role played by system boundaries: Free, completely smooth edges were found to impede the bulk magnetic susceptibility, which did not occur in the case of rough edges. That line of investigation is discussed in Chapter 5. Chapter 6 summarizes the work.

List of publications

This thesis is based on the five publications listed below, which are reproduced in Part II with kind permission of the publisher.

1. Susceptibility of the 2D spin-$\frac{1}{2}$ Heisenberg antiferromagnet with an impurity
   Kaj H. Höglund and Anders W. Sandvik
   Physical Review Letters **91**, 077204 (2003)

2. Impurity effects at finite temperature in the two-dimensional $S = 1/2$ Heisenberg antiferromagnet
   Kaj H. Höglund and Anders W. Sandvik
   Physical Review B **70**, 024406 (2004)

3. Anomalous Curie response of impurities in quantum-critical spin-$\frac{1}{2}$ Heisenberg antiferromagnets
   Kaj H. Höglund and Anders W. Sandvik
   Physical Review Letters **99**, 027205 (2007)

4. Impurity induced spin texture in quantum critical 2D antiferromagnets
   Kaj H. Höglund, Anders W. Sandvik, and Subir Sachdev
   Physical Review Letters **98**, 087203 (2007)

5. Edge effects in the two-dimensional spin-$\frac{1}{2}$ Heisenberg antiferromagnet
   Kaj H. Höglund and Anders W. Sandvik
   Physical Review B **79**, 020405(R) (2009)

Author's contribution

The author has strived for an active role in the various stages of the process leading to Papers 1–5. However, the work builds upon the ideas and suggestions of A. Sandvik, and the author's contribution is found in the implementation—planning, programming, and executing the computer simulations, analyzing data, and participating in the interpretation and reporting of the results.

Namely, in Papers 1 and 2 the author conducted the computer simulations, solved the few spin models, and wrote the drafts of the manuscripts, which were finalized together with A. Sandvik. In Paper 3 the author did most of the numerical work and wrote the draft of the manuscript, which was finalized together with the coauthor. In Paper 4 the author did the computations and participated in writing about that. The field-theoretical work was done by S. Sachdev. In Paper 5 the author did most of the numerical work and wrote the draft of the manuscript, which was finalized together with A. Sandvik, who did the analysis within the valence-bond framework.

The large scale computer simulations have utilized A. Sandvik's quantum Monte Carlo SSE algorithm, which the author has modified, when needed, to accommodate the different models considered.

Part I

Synopsis

Chapter 1

Introduction

1.1 Background and method

Many of the currently most exciting topics within the field of quantum condensed matter physics are about phenomena arising from the collective behavior of a vast number $(\approx 10^{23})$ of strongly interacting particles. High-temperature superconductivity is the most famous example. Other examples are the colossal magnetoresistance effect and heavy fermion materials, to name a few. However, in some of the cases a swift experimental progress, towards possibly very important applications, is unfortunately marred by the element of trial and error. This is because sufficient knowledge of the effective microscopic mechanisms, which give rise to the unusual macroscopic properties, is missing.[1]

A major reason for this lies in the fact that the theoretical models of strongly correlated electron systems pose formidable mathematical challenges, which mostly lack exact solutions. Existing analytical approaches, then, while relying on assumptions and approximations to some degree, may arrive at contradicting conclusions. Computational methods, on the other hand, can produce essentially exact numerical solutions—in other words, results that are unbiased—but do not on their own provide an

[1] See, e.g., Science **314**, 1072 (2006); *High T_c: The Mystery That Defies Solution* by A. Cho.

intuitive picture of the effective mechanisms involved. Most often both approaches are called for in order to shed light on the complex model systems.

The present thesis deals with the outcome of a large-scale computer simulation study with the intent to numerically address some current problems concerning the magnetic effects of defects in antiferromagnetic host systems. That high-quality numerical results can, indeed, be a most valuable complement to analytical results is exemplified in Chapters 2 and 3. The availability of bench-mark numerical data is also a prerequisite when developing alternative numerical strategies—for checking test results against—and in cases where the theoretical models have direct physical realizations the data can be compared to experimental results. A drawback of computer simulations is that they deal with finite-size systems exclusively, and that the data have to be extrapolated to the thermodynamic limit. However, as affordable computer power continues to increase, ever larger systems can be handled, and the problems previously deemed either too time consuming or too large to handle may become feasible with time.

For the numerical simulations in the present work, an established quantum Monte Carlo (QMC) method has been used—the stochastic series expansion (SSE) technique. It is one of the numerical methods available for evaluating thermodynamic expectation values for some classes of quantum lattice models. The algorithm is approximation-free: The basic idea is to first power-expand the density matrix operator, after which the partition function can be importance sampled. The algorithm and its application to models considered in the present work [2, 3] were outlined in the author's licentiate thesis [1] and will not, therefore, be repeated here. Currently, the most complete description of the method is found in Reference [4]. More background matter, references, and a very useful pedagogical tutorial can be found in the web pages[2] of A. Sandvik, who conceived the method.

[2] `http://physics.bu.edu/~sandvik/`

1.2 Model

This thesis is dedicated to the numerical study of the two-dimensional (2D) $S = 1/2$ Heisenberg antiferromagnet. It is a special case of the general Heisenberg model, which is the simplest archetypical model for microscopic magnetism: it describes the effective interaction between the spin degrees of freedom of immobile electrons. Although an old model, dating back to the early days of quantum mechanics, it is of current relevance due to the more recent discoveries of experimental strongly correlated electron systems. For example, the 2D Heisenberg antiferromagnet proved very accurate in describing the magnetic properties of the undoped parent compounds of the original high T_c copper oxide superconductors [5]. These compounds, such as La_2CuO_4, contain CuO_2 layers in which the valence electrons are found localized to the Cu sites—one-on-one—on a square lattice.

The Heisenberg model has been studied intensely for the past two decades, in a wide range of contexts and using all conceivable methods. The challenge lies in finding out what macroscopic properties the collective behavior of a large number of spins will lead to. Although no exact mathematical solution is known, the bulk physics of the 2D Heisenberg antiferromagnet, defined on a square lattice, has mostly been established [2, 5, 7–10]. For example, in determining the nature of the antiferromagnetic ground state, numerical results [6] played a vital role. Mathematically, the model is defined by the Hamiltonian

$$H = \sum_{\langle i,j \rangle} J_{ij} \mathbf{S}_i \cdot \mathbf{S}_j, \tag{1.1}$$

where $\langle i, j \rangle$ denotes a pair of nearest-neighbor spins, $\mathbf{S}_i$ is the quantum operator for the spin at location i, and J_{ij} is a coupling constant between spins i and j. For $J_{ij} > 0$ the interaction is called antiferromagnetic—neighboring spins minimize their mutual energy by pointing in opposite directions. Being the simplest model for quantum magnetism, Equation (1.1) is a reasonable and useful starting point for theoretical studies of the yet uncharted areas of strongly correlated electron physics.

One example of an emerging context for studies of strongly correlated systems is the subject of quantum phase transitions (see, for example, the textbook of Reference [11] or the review article in [12]). It is a comprehensive theoretical framework that deals with the concept of competing ground states and the corresponding elementary excitations, in order to describe the different phases of the systems. For example, in the model defined by Equation (1.1), a zero temperature phase transition can be realized by using two different nearest-neighbor couplings (J_1, J_2) in a pattern that favors singlet formation on dimers. For $J_1 \gg J_2$, say, the system is characterized by a paramagnetic ground state with a gap to particle-like $S = 1$ excitations. At some critical value of the coupling ratio $g = J_1/J_2$ the system transitions to an antiferromagnetically ordered gapless ground state with spin-wave excitations. In between these two, at finite temperatures, the quantum critical regime fans out. Here, the elementary excitations cannot be described by any simple semiclassical-like analogy [11]. The subject of quantum phase transitions is beyond the scope of this thesis but has to be mentioned because it is tangential to the present work: In Chapters 3 and 4 an impurity is utilized to probe some of the magnetic properties in the exciting quantum critical regime.

1.3 Defects

In studies of strongly correlated systems, a specific set of problems deals with the role played by defects, such as impurities and boundaries. Experimental systems consist of finite-size parts with edges of some sort, and impurities are inherent to all samples. In some cases the effect of impurities is drastic; superconductivity in the cuprates is brought on by intentional doping, which also destroys the antiferromagnetic order found in the normal state of the parent compounds. (For a review of the doping effects in the cuprates, see Reference [13]) At very low concentrations the impurities are not expected to lead to such dramatic changes, and the signal from sample edges is presumably very weak in systems with a small edge to bulk ratio. In fact, the exact extent to which minor imperfections

effect the outcome of experiments is often not known. However, small yet detectable changes in response functions due to defects can be useful too, because they inevitably reflect aspects of the host system. Hence, systematic theoretical studies of defects in prototypical model systems, such as the Heisenberg antiferromagnet, are important: For establishing the magnitude of various effects in order to interpret experimental data, as well as for shedding light on the fundamental aspects of strongly correlated states.

The strategy of using doping as a means for probing low-dimensional antiferromagnetic systems has been utilized successfully in a multitude of experiments [14–20]. For example, when nonmagnetic ions, such as Zn, are used as dilute dopants in the cuprates, NMR measurements reveal enhanced staggered magnetic moments with net $S = 1/2$ around the impurity sites in the CuO_2 planes [17–19]. This behavior has been reproduced theoretically in spin-gapped Heisenberg models, where the impurity induced moments are strongly localized [21–24]. Also in gapless systems enhanced antiferromagnetic correlations around a vacancy were observed [21, 22, 25, 26], but the spatial distribution of the impurity moment was not established in detail. For a quantum critical system, the problem had not been addressed. This, and many other aspects of the theoretical problem of a single vacancy in an antiferromagnetic background have been considered in several ground state [21–29] and finite temperature studies [23, 24, 30–35], and a coherent picture is emerging. A related problem, beyond the scope of this thesis, is the question of what happens when there is a dilute impurity concentration [36]. Some aspects have been studied, for example, by Wang and Sandvik [37], but overall sufficient numerical data as well as a general theory is missing.

In quasi-one-dimensional systems, such as the spin chain compound Sr_2CuO_3, vacancies can cut the chains into segments with free ends. The resulting boundary effects have largely been established [20, 38–41]. For example, the broad background observed in NMR spectra was accounted for by a large alternating local susceptibility, which increases in amplitude with the distance from the end of the spin chains [20, 38]. The role played by boundaries in 2D systems has not been paid much attention to.

This may partly be due to the fact that edge features are not expected to be distinguishable from the bulk signal in most experiments. However, as sample sizes approach the nanoscale, the boundary physics should become more prominent.

Recently, in a prestigious quantum field-theoretical study by Sachdev *et al.* [24], the low-temperature theory of an arbitrary quantum spin-S impurity in a 2D antiferromagnetic host system was developed. It culminated in detailed predictions for the magnetic response of the impurity, in the different finite-temperature regimes associated with a quantum phase transition occurring in the host; from a quantum disordered spin-gapped paramagnet to a gapless antiferromagnet. The said study has been a vital source of inspiration for the present work: a substantial part of the numerical investigations presented here was inspired by those far-reaching conjectures. For example, the inquiries outlined in Chapter 2 were undertaken in order to check the validity of some of the predictions. The efforts elaborated on in Chapter 3, in turn, were made to extract accurate numerical values on some quantities, which on analytical grounds had been predicted to be of importance.

1.4 Description of papers

Papers 1 and 2 report on the numerical investigations undertaken to determine the low-temperature magnetic response of a spin-S impurity coupled to an antiferromagnetically ordered 2D Heisenberg host model. The QMC results confirmed the theoretical prediction [24] of a leading-order classical-like Curie response due to alignment of the impurity moment with the local Néel order. Simple few-spin models were introduced for the sake of a simple description of this mechanism. Furthermore, the numerical data revealed that the impurity susceptibility has a subleading log diverging contribution, which was subsequently established on theoretical grounds [31, 32]. Paper 2 is a more detailed account and it considers additional impurities, such as an $S = 1$ impurity and some bond impurities as well.

Paper 3 continues with the analytical predictions of Reference [24]: in a nearly critical host the magnetic response of an impurity was predicted to have a Curie form with an anomalous (irrational) Curie constant. This view was the matter of some controversy as it had been challenged in a competing theory [29]. In order to settle the dispute, large-scale computations were performed and a value for the Curie constant was extracted. The events are discussed in Chapter 3, which also presents data for an alternate $S = 1$ impurity.

Paper 4 deals with the parallel efforts—a collaboration of numerical and analytical methods—to determine the $T = 0$ spatial magnetic distortion around the impurity in the critical 2D Heisenberg model with open boundary conditions. The uniform and staggered magnetizations were found to be delocalized across the entire sample with a universal functional form. Chapter 4 outlines those events, and also describes the fate of the magnetic structure in a magnetically ordered host system.

The question of boundary conditions had been touched upon in Paper 4. In Paper 5, the magnetic effects of free edges are investigated. Near smooth boundaries the magnetic response was found to be reduced from the bulk value, leading to an impeded overall susceptibility. This somewhat counterintuitive effect—spins along an edge should naively fluctuate more as they have fewer neighbors—was argued to be connected to enhanced antiferromagnetic correlations observed at the edges in a comblike pattern. The impeding effect was found to vanish when the boundaries were 'roughened'.

Chapter 2

Impurity susceptibility

Consider Equation (1.1) defined on a 2D square $L \times L$ lattice, where nearest-neighbor spins interact via J. With $J > 0$, attempting to minimize the energy the spins line up antiferromagnetically as $T \to 0$. For even L, the ground state is then a checkerboard of spins 'up' and 'down' with total $S = 0$ due to an equal number of spins on each sublattice. Removing or adding a single spin, for example, as shown in Figure 2.1, creates an unbalance between the number of spins on the two sublattices, which leads to a ground state with $S = 1/2$ [42] and doubly degenerate magnetization $M_z = \sum_i S_i^z = \pm 1/2$ (with respect to some quantized z-axis). The question arises; in what other ways and to what extent is the system affected by such a minute impurity? Focusing on the magnetic effects, one strategy for obtaining an answer is to determine, for example, the uniform magnetic susceptibilities of both 'pure' and defect systems, whereafter the results can be compared. Specifically, by taking the difference of the two, the so-called impurity susceptibility is obtained. The impurity effects on other quantities, such as the internal energy and specific heat, can be obtained in a similar fashion. The impurity susceptibility is defined mathematically in the next chapter. Here, the discussion is kept qualitative.

The above strategy had been used successfully by Sachdev and cowork-

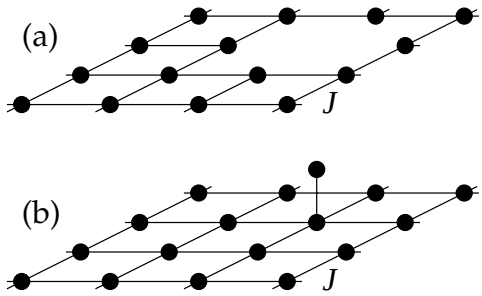

Figure 2.1: Heisenberg $L \times L$ lattices with antiferromagnetic nearest-neighbor interactions. Using even L, the models with a vacancy (a) and an off-plane added spin (b) are $S = 1/2$ impurity models due to an unpaired spin.

ers in their analytical work [24], where very detailed results for the impurity susceptibility were obtained within the broad context of quantum phase transitions. The predictions in the quantum critical regime were partly controversial [29, 43], which is the topic of Chapter 3. However, less attention had been paid to the results in the case of a magnetically ordered model. To be specific, for a spin-S impurity coupled to such a host system, as $T \to 0$ a Curie susceptibility had been obtained,

$$\chi^z_{\text{imp}} = \frac{S^2}{3T} + \frac{2}{3}\frac{C_3}{\rho_s}, \tag{2.1}$$

where ρ_s denotes the spin stiffness of the bulk-ordered antiferromagnet without impurities. The noteworthy classical-like prefactor—S^2 instead of the usual $S(S+1)$—was explained to be due to the fact that the impurity spin 'gets stuck' to the evolving local magnetic order at low T and, therefore, it behaves like a classical magnetic moment. A universal value was proposed for the constant C_3.

Very much motivated by the elegant analytical work, we carried out finite-T quantum Monte Carlo simulations in order to check some of the predictions. The events are reported on in detail in Paper 1. In brief,

we considered the $S = 1/2$ Heisenberg antiferromagnet on a 2D periodic lattice with either a vacancy or an added spin impurity. The numerical results obtained for the impurity susceptibility confirmed the predicted [24] leading-order Curie prefactor for both impurity types. For a simple explanation of this 'classical-like' behavior, we constructed toy models—highly simplified few-spin effective impurity models—which were able to reproduce the numerical results. Very recently, a detailed theoretical analysis of the the leading-order behavior was conducted by others [35].

However, the data for the impurity susceptibility was observed to also contain a low-T logarithmically divergent subleading contribution. This behavior had not come up on analytical grounds, although a similar trend had, in fact, been observed in a previous Green's function study [26], and a kind of anomaly had also been observed for the case of a finite impurity concentration [36]. Ensuing theoretical efforts [31, 32], to explain our numerical findings, found, indeed, a previously unnoticed log divergent contribution. In a nonlinear σ model study [31] the impurity susceptibility was rewritten,

$$\begin{aligned} \chi^z_{\text{imp}} &= \frac{S^2}{3T}\left[1 + \frac{T}{\pi\rho_s}\ln\left(\frac{C_1\rho_s}{T}\right)\right. \\ &\quad \left. - \frac{T^2}{2\pi^2\rho_s^2}\ln\left(\frac{C_2\rho_s}{T}\right) + O\left(\frac{T}{\rho_s}\right)^3\right], \end{aligned} \tag{2.2}$$

where the unknown constants $C_{1,2}$ are in general nonuniversal, but become universal when a quantum critical point is approached. To the first subleading term $\propto \ln(1/T)$, which accounts for the log divergence, the universal prefactor $S^2/3\pi\rho_s$ was assigned. By adjusting the constants $C_{1,2}$, we verified that the new prediction agreed with our QMC data. An alternative theory [32] was also qualitatively in line with the new results.

Encouraged by the course of events, we delved deeper into the numerical investigations of the impurity problem, as reported on in Paper 2. Two-vacancy models were considered, as well as a single vacancy in the 3D model, for which some analytical predictions had been made [32]. Also, a novel impurity model was constructed; a spin coupled ferromag-

netically to its four nearest neighbors on the square lattice, with an expected $S = 1$ impurity moment. In this case also, the QMC data confirmed the predicted leading-order Curie prefactor, as well as the universal form of the first subleading log divergent contribution. Effectively frustrating ferromagnetic interactions between nearest-neighbor spins at the Cu sites had been suggested [45] to result from hole doping the parent cuprate compounds. Therefore, we considered an impurity model with a single frustrating ferromagnetic bond on the square lattice, and compared it to a missing-bond model. In addition to calculating the impurity susceptibilities, some impurity effects on the specific heat and the internal energy were also determined. The effective-model concept was developed to some degree in Paper 2.

Chapter 3

Anomalous Curie response

In this Chapter, Equation (1.1) is applied to a periodic $L \times L$ bilayer lattice as shown in Figure 3.1 (a). The Heisenberg Hamiltonian becomes

$$H = J \sum_{\langle i,j \rangle} \mathbf{S}_{1,i} \cdot \mathbf{S}_{1,j} + J_\perp \sum_i \mathbf{S}_{1,i} \cdot \mathbf{S}_{2,i}, \tag{3.1}$$

where the intra- and interlayer coupling constants are J and $J_\perp$, respectively. The indices 1 and 2 refer to the bottom and top layers, respectively. Because there are intralayer couplings only in the bottom layer (a Kondo lattice), the model will be referred to as the incomplete bilayer, which the main results in this chapter are for. The closely related symmetric bilayer has interactions J in both layers.

The antiferromagnetic bilayer models have attracted some attention, not the least because they can be used to study quantum phase transitions [43, 46–58]. When $J_\perp \gg J$, adjacent interlayer spins tend to form singlets at low T, whereas for $J_\perp \ll J$ the antiferromagnetic order dominates among the spins that interact by J. The ratio $g = J_\perp / J$ serves as the parameter that sets the phase of the model: A critical value $g = g_c$ separates the gapless Néel ground state with spin-wave excitations for $g < g_c$ from the spin-gapped disordered ground state with $S = 1$ excitations for $g > g_c$. In our calculations we used $g_c = 1.3888(1)$ for the incomplete

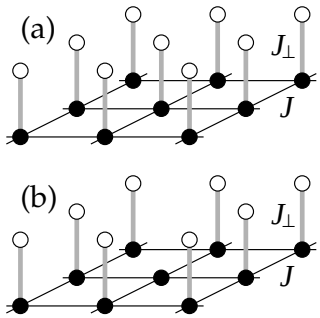

Figure 3.1: Incomplete bilayer lattice with $L = 3$. Nearest-neighbor interactions J between bottom layer spins (black) are absent among the top layer spins (white). Interlayer couplings $J_\perp$ are shown as grey. By removing a single spin from the intact model (a), an $S = 1/2$ impurity model (b) is obtained.

bilayer model [$g_c = 2.5220(3)$ for the symmetric bilayer] [56], which at finite temperatures gives a nearly quantum critical system.

3.1 $S = 1/2$

In Figure 3.1 (b), a single spin has been removed from the top layer of the incomplete bilayer model. This effectively creates an $S = 1/2$ impurity as there is an unpaired spin in the opposite layer. As in the previous Chapter, the question is; how does the single impurity alter the bulk response of the almost critical host model, or, conversely; what is the susceptibility of the impurity itself? In order to answer that question, addressed in Paper 3, the total susceptibilities of the critical systems with and without vacancy were computed. They are defined as

$$\chi_k^z = \frac{J}{T} \left\langle \left(\sum_{i=1}^{N_k} S_i^z \right)^2 \right\rangle, \tag{3.2}$$

with $k = 0$ for the intact model ($N_0 = 2L^2$) and $k = 1$ for the model with the vacancy ($N_1 = 2L^2 - 1$). The difference between the two defines the impurity susceptibility

$$\chi^z_{\text{imp}} = \chi^z_1 - \chi^z_0. \tag{3.3}$$

As χ^z_{imp} is the difference between two extensive quantities, which should only differ with respect to the effects originating from the single vacancy, it follows that very precise data for the individual susceptibilities are called for. The use of improved estimators [59] is crucial.

In the field-theoretical work by Sachdev *et al.* [24], the impurity response in an antiferromagnetic host system had been considered in a broad context. For the impurity susceptibility a Curie form had been found— $\chi^z_{\text{imp}} \sim C/T$ as $T \to 0$—with the Curie constant taking different values depending on the parameter g:

$$C = S^2/3, \qquad g < g_c, \tag{3.4}$$

$$C = C^* = \tilde{S}(\tilde{S}+1)/3, \;\; \tilde{S} \neq S, \qquad g = g_c, \tag{3.5}$$

$$C = S(S+1)/3, \qquad g > g_c, \tag{3.6}$$

where $\hbar = k = 1$. For $g < g_c$, that is, in the magnetically ordered regime, the classical-like Curie constant [S^2 instead of $S(S+1)$] we had confirmed numerically up to a log correction (Chapter 2). In a paramagnetic system, $g > g_c$, the usual prefactor is due to the strongly localized impurity moment in the spin-gapped state. The most remarkable prediction was for $g = g_c$; the critical Curie constant takes a universal and irrational value in the range $S^2/3 < C^* < S(S+1)/3$. For $S = 1/2$ we get $1/12 < C^* < 1/4$. Moreover, according to Equation (3.5), the effective impurity spin $\tilde{S} \neq S$ is neither integer nor half-integer but most likely irrational. However, these remarkable results had been challenged in a competing Green's function theory [29], which claimed that $\tilde{S} = S$ and, hence, $C^* = C = 1/4$ (for $S = 1/2$). A previous numerical study [43] had left the matter unsettled.

Next, the numerical data for the impurity susceptibility are presented, from which the critical Curie constant is obtained according to,

$$C^* = \lim_{T \to 0} T\chi^z_{\text{imp}}. \tag{3.7}$$

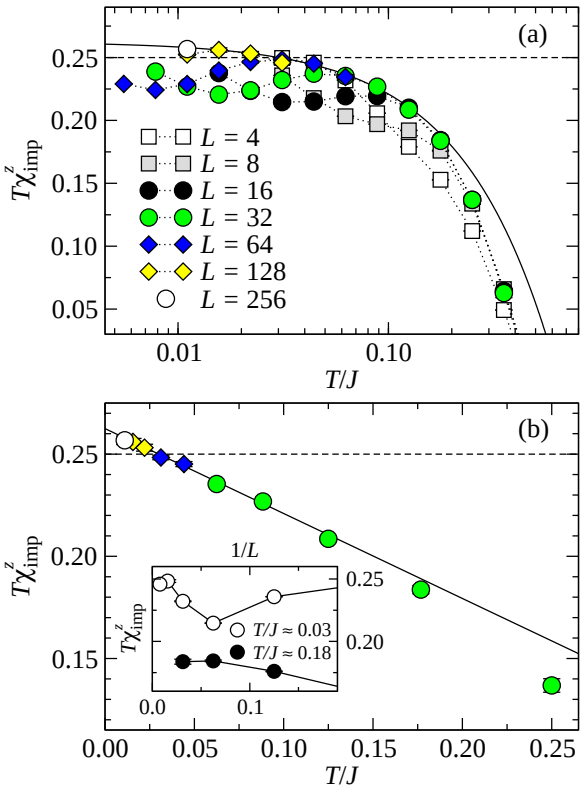

Figure 3.2: QMC results for $T\chi^z_{imp}$ for an $S = 1/2$ vacancy in the incomplete bilayer. Panel (a) uses lin-log axes and shows results for different L. Only size-converged data are shown in panel (b), where lin-lin x axes are used and the straight line is a linear fit to the low T data. The inset shows size convergence of results at two different T.

Figure 3.2 (a) shows QMC data for the temperature dependence of $T\chi^z_{\rm imp}$ for different system sizes L. At high T the spins are independent and each contribute $1/4T$ to the total susceptibilities. Since there is one less spin in

the impurity model than in the intact system, the trend $T\chi^z_{\rm imp} \to -1/4$ as $T \to \infty$ is obtained (although not explicitly shown in the Figure). Moving towards lower T, the data for smaller systems deviate from those of larger L due to finite-size effects. In the limit $T \to 0$, one always gets $T\chi^z_{\rm imp} \to +1/4$ for any L, due to the $S = 1/2$ ($S = 0$) ground state of the impurity (intact) model. At intermediate T a local minimum is observed in the finite-size behavior for $L \geq 16$. Size-converged data, that is, results representative of an infinite-size system, are obtained when data for L and $L/2$, at given T, agree within statistical errors. Such data are shown exclusively in Figure 3.2 (b), with examples of the size-convergence shown in the inset. At low temperatures a linear behavior is observed and extrapolation gives $C^* = 0.262(2)$. That the value exceeds $1/4$, although only by roughly 5%, is solid numerical support for the notion of an anomalous Curie response, as predicted by theory in Reference [24]. That the value does not fit within the conjectured range $[1/12, 1/4]$ need not be viewed as a controversy: The suggested range merely reflected a simplest intuitive scenario [60]. In fact, C seems to be a nonmonotonous function of g.

In order to test the prediction of universality, that is, that the details of the host are irrelevant for C^*, the calculations were repeated for the symmetric bilayer with an $S = 1/2$ vacancy. The results were found to agree with those of Figure 3.2, but the numerical precision was insufficient for an independent extrapolation of C^*. The symmetric bilayer has a higher critical ratio $g_{\rm c}$ and double the number of interactions J compared to the incomplete bilayer. Therefore, it is roughly twice as demanding computationally.

3.2 $S = 1$

Next, results are shown for an impurity model with $S = 1$. Such models can be realized, as shown in Figure 3.3, by making (a) one of the interlayer couplings in the incomplete bilayer ferromagnetic, $J_\perp \to -J_\perp$. In the symmetric bilayer, this has to be done to all five couplings to a given

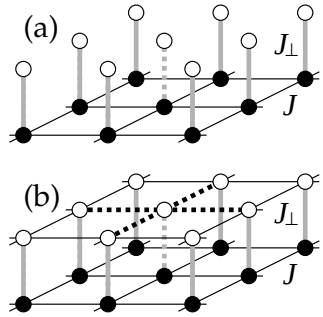

Figure 3.3: $S = 1$ impurity models are obtained by turning a single interlayer coupling in the incomplete bilayer (a) and all five couplings to a given spin in the complete bilayer (b) into ferromagnetic ($J_\perp \rightarrow -J_\perp$), as shown with the dashed lines.

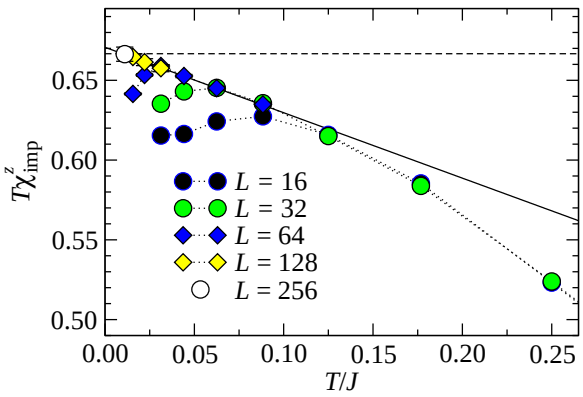

Figure 3.4: QMC data for the impurity susceptibility of an $S = 1$ impurity in the incomplete bilayer. The line is a linear fit to the size-converged low T data.

spin, as shown in Figure 3.3 (b). In both cases the finite-size impurity systems lock into a $S = 1$ ground state as $T \to 0$. The latter model was considered in Paper 3, where the estimate $C^* = 0.663(2)$ was obtained in the same manner as previously described. This value is slightly below the 'normal' value $2/3$, but the discrepancy was found to be too small (compared to the statistical error) to be conclusive. Figure 3.4 shows previously unpublished results for the model in Figure 3.3 (a). The high- and low-T finite-size behaviors are understood in the same manner as for the $S = 1/2$ impurity model. At low T the size-converged data again become linear in T (some finite-size effects are also shown). Extrapolation gives $C^* = 0.671(2)$, which in this case is slightly above $2/3$. Hence, higher precision is required to definitely settle the fate of the $S = 1$ impurity. However, what the results do show is that the anomaly is smaller than for an $S = 1/2$ impurity.

This Chapter is concluded with a specific detail extracted from the high-precision data underlying the results discussed above. According to the theory of the nonlinear σ model [10], a critical system should exhibit a universal linear low-T behavior in $\chi_0^z(T)$, with intercept 0. This feature had been confirmed [48, 53, 54] for the intact (without impurity) symmetric bilayer. However, for the incomplete bilayer a weak curvature had been observed in a comparable temperature range $[0.05, 0.2]$ [57]. Although not shown here, our QMC data reproduced that feature, but at still lower $T \in [0.01, 0.07]$ a linear $\chi_0^z \to 0$ as $T \to 0$ behavior was, indeed, observed [61].

Chapter 4

Magnetization distribution

This Chapter continues with the model familiar from the previous Chapter; the incomplete bilayer with a vacancy [Figure. 3.1 (b)]. Due to an odd number of spins left, the ground state in the finite L system has $S = 1/2$. The positive sector of the $M_z = \sum_i S_i^z = \pm 1/2$ doubly-degenerate ground state is considered here. The questions addressed in this Chapter are; how is the $T = 0$ magnetization spatially distributed in the system, and what is the influence of the phase of the host? In the spin-gapped state, $g > g_c$, the magnetic distortion is known to be found exponentially close to the impurity, with the localization length scale set by the inverse of the spin gap [21–25]. Hence, the effective behavior of a localized impurity moment. For a Néel ordered model, $g < g_c$, some results had appeared [22, 62], but for $g = g_c$, that is, in the quantum critical phase, the issue had not been dealt with. We used Equation (3.1) with $J_\perp/J = g = g_c = 1.3888(1)$ [56].

4.1 Quantum critical model

For odd L, a vacancy can be placed at the exact center of the $L \times L \times 2$ lattice. Using free edge, or open, boundary conditions, the spins at the end of rows see no neighbors in that direction. In this way, the ground state

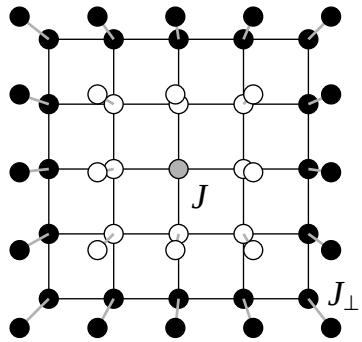

Figure 4.1: Top view of an $L = 5$ incomplete bilayer model with a vacancy. Free edge boundary conditions are used. The center gray spin constitutes 'frame' $R = 0$. The white and black spins belong to frames $R = 1$ and 2, respectively. An analogous frame decomposition can also be applied to a single layer model.

magnetization can be studied using the strategy of Reference [22]: The lattice surrounding the vacancy is decomposed into 'frames', as shown in Figure 4.1. For each frame index R, which labels the distance from the center, the uniform and staggered magnetization components are defined, respectively,

$$M_0(R) = \left\langle s \sum_{i \in R} (S^z_{1,i} + S^z_{2,i}) \right\rangle, \tag{4.1}$$

$$M_\pi(R) = \left\langle s \sum_{i \in R} (-1)^{x_i + y_i} (S^z_{1,i} - S^z_{2,i}) \right\rangle, \tag{4.2}$$

with the same notations as earlier. The factor $s = 2M_z = \pm 1$ is included in order to make the contributions positive for both $M_z = \sum_i S^z_i = \pm 1/2$ states. The corresponding integrated magnetizations are given by

$$I_k(R) = \sum_{r=0}^{R} M_k(r), \tag{4.3}$$

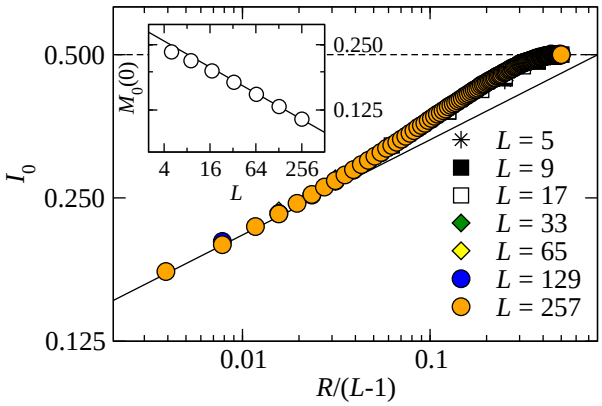

Figure 4.2: QMC data for the integrated uniform frame magnetization shown on log-log axes. The $L = 257$ results almost completely hide smaller L data because of the tight data collapse. The exponent η', which is obtained from the power-law behavior observed for the $R = 0$ magnetization shown in the inset, solely governs the spatial magnetic structure, including I_0.

where $k = 0$ or π. Of special interest is $I_0(R)$, which has to be exactly $1/2$ at the edge of the lattice, that is, for $R_{\max} = (L-1)/2$. The expectation values in Equations (4.1), (4.2), and (4.3) were calculated for each L considered, at sufficiently low $T > 0$ to ensure negligible temperature effects.

Figure 4.2 shows QMC data for the integrated uniform frame magnetization I_0, for different L, against $R/(L-1)$ on log-log axes. The L dependent data is observed to collapse tightly onto a single curve, and a power-law behavior is observed for small R/L. From the concurrent field-theoretical efforts by Sachdev, predictions for the spatial scaling forms were obtained: In the $R/L \to 0$ limit, that is, far from the impurity and system edges, both the uniform and the staggered magnetizations should obey a power-law behavior governed by a single exponent η'. For in-

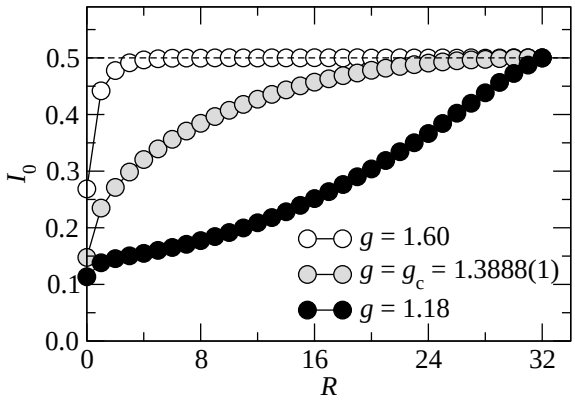

Figure 4.3: $L = 65$ results for the incomplete bilayer with a vacancy. $I_0(R)$ data for different values on the tuning parameter g are compared.

stance,

$$I_0(R) \propto \left(\frac{R}{L}\right)^{\eta'/2}. \tag{4.4}$$

Using the $R = 0$ data, shown in the inset of Figure 4.2 [$I_0(0) = M_0(0)$], the estimate $\eta' = 0.40(2)$ was obtained from the relation $I_0(0) \propto L^{-\eta'/2}$. That value has been used for the line in the main panel, and it was found to work also for the staggered quantities, as predicted by Sachdev. A numerical estimate in agreement with our η' had, in fact, been obtained previously in a time dependent context [43]. However, that the same exponent would also govern the spatial impurity effects had not been anticipated. The theory part of the matter was later developed in detail in a study by Metlitski and Sachdev [63].

In Figure 4.3, $L = 65$ results for $I_0(R)$ for different g are compared. The power-law behavior found for the critical results (gray symbols) indicates that the magnetic distortion is delocalized over the entire system. For example, at the impurity site, $M_0(0, g = g_c) \to 0$ as $L \to \infty$. In contrast, for $g > g_c$ (white symbols) the total $S = 1/2$ magnetization is

localized exponentially close to the impurity (within frame $R \approx 8$ in Figure 4.3) and $M_0(0, g > g_c)$ converges rapidly, with increasing L, to a g dependent constant value. In the Néel phase (black symbols), addressed in more detail in the next Section, the situation appears ambiguous: For any L, I_0 becomes $1/2$ only at the very edge of the lattice, while $M_0(0, g < g_c)$ seems to converge to an almost g independent positive constant m_0, say, as $L \to \infty$. This would point to a scenario where part of the ground state magnetization is localized to the impurity and the rest is spread out over the entire sample. In fact, the nonmonotonous behavior of $M_0(0)$ as a function of g somewhat resembles the one found for the Curie constant in the previous Chapter.

4.2 Néel ordered model

Next, the ground state magnetic structure in a Néel ordered model is determined. To that end, the Heisenberg Hamiltonian is applied to an $L \times L$ single-layer lattice,

$$H = J \sum_{\langle i,j \rangle} \mathbf{S}_i \cdot \mathbf{S}_j. \tag{4.5}$$

By choosing L odd (which gives odd $N = L \times L$), the ground state has the magnetization $|M_z| = |\sum_{i=1}^{N} S_i^z| = 1/2$ and, hence, no actual impurity is needed in this case. Open boundary conditions are used. The R dependent expectation values defined in Equations (4.1), (4.2), and (4.3) are computed as previously for the critical model.

The inset of Figure 4.4 shows $L = 33$ QMC data for the uniform frame magnetization. Apart from the markedly higher value at $R = 0$, $M_0(R)$ is observed to grow roughly linearly with R, with a slight decrease for larger R. For the magnetization at the center of the lattice ($R = 0$), the result $M_0(0) \to m_0 = 0.099(1)$ as $L \to \infty$ is obtained. Only a few frames away from the sample edge, an oscillating behavior escalates rapidly to a maximum at $R = R_{\max}$. The consequences of the edges are discussed in Chapter 5, here focus is on the large R and small R/L results, that is,

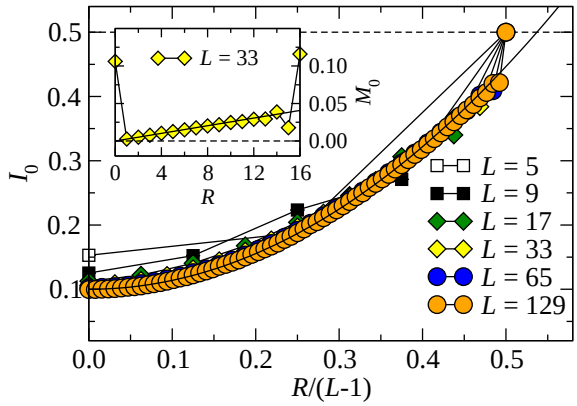

Figure 4.4: Uniform magnetization distribution in the single layer, magnetically ordered, Heisenberg antiferromagnet. Symbols show QMC data and the curves are the functions of Equations (4.6) and (4.7)

far away from the system center and edges. Although not shown, when plotted against $R/(L-1)$ the LM_0 data for different systems L collapse onto a single curve (apart from the behavior at $R = 0$ and very close to the lattice edges). Hence, neglecting higher-order terms that appear to be small, one is led to the relation,

$$M_0(R)L = c_0 \left(\frac{R}{L}\right), \tag{4.6}$$

with $c_0 = 2.77(2)$ as the best estimate. The corresponding integrated quantity should then be,

$$I_0(R) = \frac{c_0}{2}\left(\frac{R}{L}\right)^2 + m_0, \tag{4.7}$$

which agrees with the QMC results, as shown by the curve in the main panel. Equations (4.6) and (4.7) are primarily for small R/L, but they are quite accurate across the whole sample, as seen in Figure 4.4.

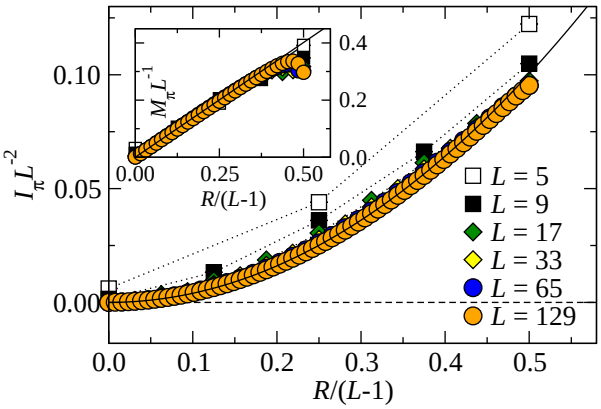

Figure 4.5: Spatial distribution of the staggered magnetization in the single layer Heisenberg antiferromagnet.

Figure 4.5 shows the spatial distribution of the staggered component, as obtained in our QMC simulations. Apart from minor finite-size effects for small systems, a data collapse is obtained by normalizing M_π and I_π with L^{-1} and L^{-2}, respectively. For the line in the inset and the parable in the main panel, we have used the expressions,

$$M_\pi(R)L^{-1} = c_\pi \left(\frac{R}{L}\right), \tag{4.8}$$

$$I_\pi(R)L^{-2} = \frac{c_\pi}{2}\left(\frac{R}{L}\right)^2, \tag{4.9}$$

where $c_\pi = 0.803(2)$.

Chapter 5

Edge effects

In numerical studies of spin lattice models, it is common practice to use periodic boundary conditions in order to avoid effects stemming from the system edges. An expected benefit is usually a faster convergence of the system size (L) dependent data to the bulk limit $L \to \infty$. Analytical studies, on the other hand, consider infinite systems or also use periodic boundary conditions. Why explicit edge studies have mostly been neglected so far, may partly be due to the fact that in most experimental contexts the possible edge effects are not expected to be relevant. An exception are the quasi-1D systems, such as Sr_2CuO_3, where experimental effects of open-end spin chains have been established theoretically [38–41]. In 3D and 2D systems, the effects from sample boundaries may not be distinguishable from the bulk signal because of the small edge to bulk ratio. However, with a further sample miniaturization the boundary physics may become important.

In the latter part of the previous Chapter, the Heisenberg antiferromagnet, Equation (4.5), was considered. Open boundary conditions and odd L were used in order to study how the ground state magnetization is distributed on the $L \times L$ lattice, mainly far away from the boundaries and center. In this Chapter, focus is on the edges. In order to investigate how the boundary conditions affect the magnetic susceptibility of the bulk, ob-

tained for a periodic model, finite-T QMC simulations were performed. Using even L, the total magnetization $M_z = \sum_i S_i^z \to 0$ as $T \to 0$, and the $1/T$ divergent low T susceptibility associated with $M_z = \pm 1/2$ is avoided. Both semiopen and completely open systems, shown in Figures 5.1 (b) and (c), respectively, were considered. The obvious difference between the two is that the latter model has corners, which may give rise to additional effects, possibly interesting in their own right.

5.1 Negative edge susceptibility

To start with, the individual uniform magnetic susceptibilities were computed,

$$\chi_k = \frac{J}{T} \left\langle \left(\sum_{i=1}^{N} S_i^z \right)^2 \right\rangle, \tag{5.1}$$

where k is the number of open edges; $k = 0$ for the periodic system, and $k = 2$ and 4 for models with semiopen and fully open boundaries, respectively. In analogy with the impurity susceptibility of Chapter 3, an edge susceptibility can be defined,

$$\chi_{\mathrm{E}} = (\chi_k - \chi_0) / kL, \tag{5.2}$$

where the normalizing constant in the denominator is included because the difference in the responses is expected to scale with the total length kL of the free edges. A first guess would be $\chi_{\mathrm{E}} > 0$, that is, the 'dangling' edge spins should enhance the susceptibility and, hence, $\chi_k > \chi_0$. Surprisingly, at low temperatures this intuition turns out to be wrong.

Figure 5.2 shows QMC data for χ_{E} as a function of T/J for a semiopen system. The fact that the results for different L are observed to coincide as L grows, confirms the scaling assumption of Equation (5.2). At high T/J, χ_{E} vanishes because there is an equal number of independent spins in both periodic and free-edge models. In the limit $T/J \to \infty$ we always eventually get $\chi_{\mathrm{E}} \to 0$ (seen explicitly for $L = 4$ and 8) due to the singlet ground state of even L models. That the data don't change with

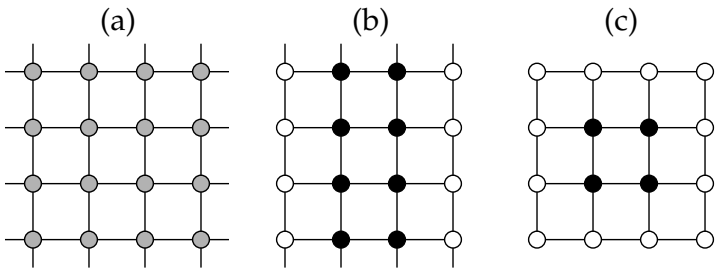

Figure 5.1: Single layer lattices with $L = 4$. Using periodic boundary conditions (a), all spins are equal. In the models with semiopen (b) and open (c) boundary conditions, the white and black spins are at distances $R = 0$ and $R = 1$ from the system edge, respectively.

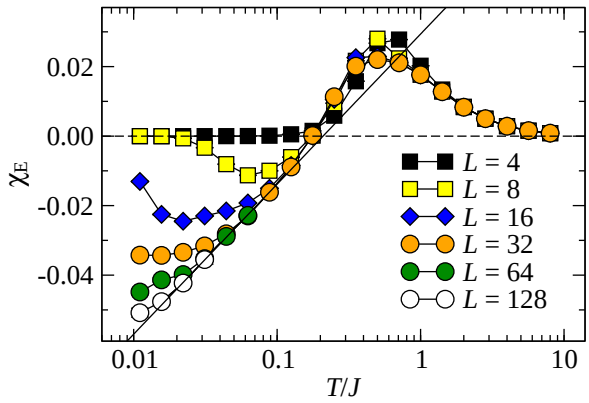

Figure 5.2: Temperature dependence of the edge susceptibility for a semiopen system, using lin-log axes. Errorbars are smaller than symbols. The line shown in the lin-log plot is a log fit to size-converged low T data

increasing L is, once again, used as the criterium for size convergence. Tracing the size-converged data from high towards lower temperatures, the values increase (reaching a maximum at $T/J \approx 0.5$) just as anticipated on behalf of more susceptible edges. However, continuing towards still lower T/J, the edge response decreases and, in fact, becomes negative in a fashion consistent with $\chi_{\mathrm{E}} \propto -a \log(J/T)$. For the line in Figure 5.2, which uses lin-log axes, $a = 0.019$ has been used.

The calculations were repeated for the classical Heisenberg antiferromagnet, that is, the $O(3)$ σ model. In that case χ_{E} was observed to converge, as $L \to \infty$, to a roughly T independent positive constant. Hence, the negative edge susceptibility, as observed for the quantum model, is somewhat surprising, not the least when contrasted to the one found for the single-impurity susceptibility (Chapter 2); a $1/T$ divergence with positive log corrections as $T \to 0$. Although not shown, the QMC data obtained for a fully open system completely overlap the semiopen results for large L. Therefore, system corners seem to be irrelevant for χ_{E} in the thermodynamic limit. (The effect per spin, $L^{-2}\chi_{\mathrm{E}} \to 0$, as $L \to \infty$.)

The uniform susceptibility of Equation (5.1) can be resolved spatially by computing the response at site i,

$$\chi_k(i) = \beta \langle S_i^z M_z \rangle, \tag{5.3}$$

with $\sum_i \chi_k(i) = \chi_k$. In a periodic model the location i is irrelevant; $\chi_0(i) = \chi_0/L^2$. In a semiopen system the local response will depend only on the perpendicular distance R from a free edge, $\chi_2(i) = \chi_2(R)$ (because the lattice has translational invariance in the parallel direction). At the edge we define $R = 0$, and as one moves away from it, $R = 1, 2, \ldots$, as illustrated in Figure 5.1. In analogy with Equation 5.2, the position dependent edge susceptibility is defined,

$$\chi_{\mathrm{E}}(R) = \chi_2(R) - \chi_0/L^2. \tag{5.4}$$

Figure 5.3 shows $L = 64$ QMC data for $\chi_{\mathrm{E}}(R)$ at two different temperatures for which results are roughly size-converged. At $\beta = 1$ (a temperature for which $\chi_2 > \chi_0$ in Figure 5.2) one can see that the edge spins

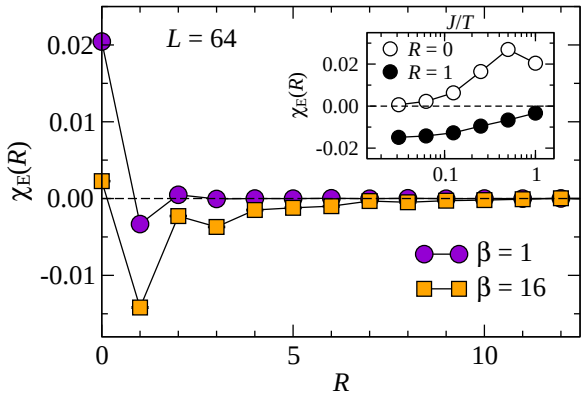

Figure 5.3: Position dependent edge susceptibility at distance R from the free edge of a 64 × 64 semiopen lattice. Inset shows how the $R = 0, 1$ data evolve with temperature.

($R = 0$) are, indeed, more susceptible than bulk spins at this temperature. However, as the temperature is lowered $\chi_{\mathrm{E}}(0)$ seems to go to zero, as observed in the inset. In fact, to some surprise one finds that it is mainly the spins next to the free edges, $R = 1$, that are responsible for the negative edge susceptibility at low T. The available data also suggest that the response remains reduced for several R away from the edges.

5.2 Knight shift consequences

The site dependent susceptibility $\chi_2^z(i)$ of Equation. (5.3) can, in principle, be obtained experimentally [20, 34]. The spectrum from a NMR measurement represents the frequency distribution function of the Knight shift, which is caused by the hyperfine interaction between nuclear and electronic spins and is, hence, proportional to the local response. For the

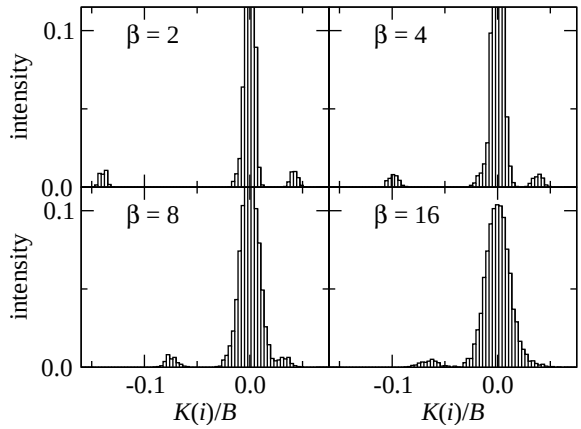

Figure 5.4: Knight shift distribution at different β, as obtained from QMC data for $L = 64$. The cumulative histogram is normalized to one.

Knight shift at site i one can use the expression [64],

$$K(i) = A_{\|}\chi_2(i) + B\sum_{\delta}\chi_2(i+\delta), \tag{5.5}$$

with $A_{\|} = -4B$ as an experimentally determined approximate relation for Cu NMR. The first term is due to the onsite hyperfine coupling and the sum is taken over the nearest neighbors, which are four for bulk spins but three for edge spins in the semiopen model. The temperature evolution of the distribution function for $K(i)/B$ is shown in Fig. 5.4. The large center peak at $K(i) = 0$ is seen to broaden as the temperature is lowered, which is due to increasing site-to-site fluctuations in the response of the bulk spins away from the edges. In addition, two 'bumps' of roughly equal intensities are observed on both sides. The one to the left should stem from the edge spins ($R = 0$), which, although more susceptible at high T/J, assume the bulk response at low temperatures, as previously discussed. Hence, the bump is observed to move towards the center peak as the temperature is lowered. In the same process, the center peak is

seen to devour the rightmost bump, which, in turn, should be due to the spins next to the free edges ($R = 1$), for which the reduced response was found compared to the bulk value. Whether these distinct edge features can be observed experimentally is questionable. Samples consisting of extremely small fragments are probably required to distinguish any edge effects from the bulk signal. What is more, the fragments are probably of irregular shapes and have uneven, or rough, edges.

As a first step towards a possibly more realistic description, models with rough boundaries were realized in the following manner. While traversing the edges of a fully open lattice, each edge spin is either removed, coupled to an extra off-lattice spin, or simply left alone with equal probability 1/3. In order to still have a ground state with $S = 0$, the roughness was executed in a way that conserves the number of spins on the two sublattices. The QMC data obtained for $\chi_{\mathrm{E}} = (\chi_4 - \chi_0)/4L$, averaged over several hundred of random edges, were presented in Paper 5. The results show, that in this case the size-converged data are consequently positive, with a possible log divergent behavior. Hence, boundaries can clearly have a profound impact: For the case of uneven boundaries the intuition of dangling edge spins seems to be correct. In the limit when the edges are made fully smooth, the negative edge susceptibility should be recovered. Others have embarked on systematic investigations into the boundary roughness effects [65].

5.3 Spin correlations

It may be recalled from Chapter 1 that the enhanced antiferromagnetic spin correlations surrounding a vacancy in an antiferromagnetic host are accompanied by a classical-like impurity susceptibility with nontrivial log corrections. In a periodic 2D lattice, a vacancy constitutes a sort of a 0D boundary. Hence, one is tempted to suspect that the puzzling negative edge susceptibility is linked to altered spin correlations, of some kind, near the open boundaries.

To look into this matter, the nearest-neighbor spin correlations were

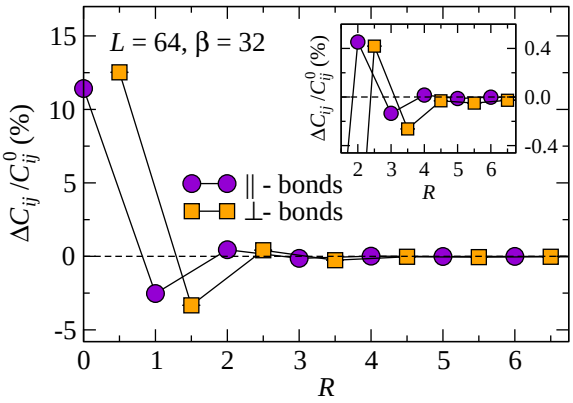

Figure 5.5: The relative deviation of the nearest-neighbor correlations C_{ij} from the bulk value C^0_{ij} is position (R) dependent. The QMC data is for a 64×64 semiopen system at $\beta = 32$. Integer and half-integer R are for bonds ij parallel and perpendicular to the free edge, respectively. The inset is a magnification of the $R \geq 2$ results.

computed,

$$C_{ij} = |\langle \mathbf{S}_i \cdot \mathbf{S}_j \rangle|, \tag{5.6}$$

and then they were compared to the bulk value C^0_{ij}. The deviation $\Delta C_{ij} = C_{ij} - C^0_{ij}$ should depend on R; integer and half-integer values for pairs ij parallel and perpendicular to the free edges, respectively, were used. Figure 5.5 shows QMC results for the relative deviation $\Delta C_{ij}/C^0_{ij}$ for a 64×64 semiopen lattice at inverse temperature $\beta = 32$. It is seen that the nearest-neighbor correlations of pairs ij along the the edge, $R = 0$, and the first rung, $R = 0.5$, are enhanced by more than 10%. Moving to the next spin line ($R = 1$) and rung ($R = 1.5$), the correlations are negative (reduced from the bulk value) by a few percent. Moving one more step away from the edge, the comblike pattern of enhanced correlations is repeated, as shown in the inset. For $R \geq 4$, the deviations seem to decay rapidly to zero.

In conclusion, in Paper 5 the comblike pattern was reproduced by performing a variational valence-bond analysis. It was argued that the increased tendency to local singlet formation on dimers is at the heart of the negative edge susceptibility. In a concurrent field-theoretical study [66], the observed correlation pattern was found to be purely a quantum effect, and the negative edge response was explained to originate from low-lying spin waves. The prefactor of the log divergence observed in the QMC data of Figure 5.2 agrees reasonably with the analytical prediction [66].

Chapter 6

Summary

This thesis has accounted for a numerical study of the 2D $S = 1/2$ Heisenberg antiferromagnet. In order to determine some of the magnetic effects brought about by defects, such as single impurities and system boundaries, large-scale quantum Monte Carlo computer simulations were performed.

Part of the problems addressed in this work originates from analytical studies, which, in the case of strongly correlated quantum systems, rely on assumptions and approximations to some degree. One intention of the computational investigations presented here has been to produce unbiased high-quality numerical data against which such predictions can be tested.

For a spin-S impurity coupled to a magnetically ordered host model, a predicted [24] classical-like leading-order Curie susceptibility was numerically confirmed [Paper 1, Paper 2]. In addition, the QMC data revealed a $T \to 0$ divergent contribution, which was subsequently established on theoretical grounds [31, 32]. For a nearly quantum critical Heisenberg model, the Curie prefactor of the impurity susceptibility was numerically obtained [Paper 3]. The fact that the value turned out to be anomalous, in the sense that it corresponds to irrational S, settled an analytical disagreement [24, 29]. Furthermore, in a joint analytical and numeri-

cal study [Paper 4], the spatial distribution of the impurity moment was found to span the entire, nearly critical, host system. Finally, the influence of system edges was examined [Paper 5]. Open boundary conditions (smooth edges) were found to impede the bulk susceptibility; particularly the spins close to the edges were observed to have a reduced magnetic response compared to bulk spins. In contrast, uneven (or rough) edges were found to enhance the susceptibility. Based on these initial numerical findings, the edge effects were examined on analytical grounds by others [66].

In studies of strongly interacting systems, slight defects, such as single impurities, have successfully been used in many previous studies to probe various aspects of the complex host systems. This work has adapted this strategy, using a powerful and established numerical procedure, to carry out investigations concerning aspects of the magnetic response of the impurities. Impurity studies analogous to those presented here should, in turn, be useful when applied to other relevant models, and such problems have already been addressed by others [67].

It is obvious that theoretical single impurity problems cannot be directly related to the physics of a many spin system with, for example, a finite impurity concentration, which clearly is an important, yet highly challenging vista to explore. Sufficient numerical data for that problem is currently missing. Also, systematic numerical investigations concerning the effects of system boundaries, such as rough edges, should be important from an experimental viewpoint. However, a detailed knowledge of the behavior of one impurity should, at least in a naive sense, be a prerequisite for understanding the effects of many impurities. To that end, as an invaluable complement to analytical studies, computational strategies have proved quite powerful and the numerical results vital.

Bibliography

[1] Kaj Höglund, *Numerical studies of impurity effects in the 2D Heisenberg antiferromagnet*, Licantiate thesis, Åbo Akademi University, 2004.

[2] A. W. Sandvik, *Finite-size scaling of the ground-state parameters of the two-dimensional Heisenberg model*, Phys. Rev. B **56**, 11678 (1997).

[3] A. W. Sandvik, *Stochastic series expansion method with operator-loop update*, Phys. Rev. B **59**, R14157 (1999).

[4] O. F. Syljuåsen and A. W. Sandvik, *Quantum Monte Carlo with directed loops*, Phys. Rev. E **66**, 046701 (2002).

[5] E. Manousakis, *The spin-1/2 Heisenberg antiferromagnet on a square lattice and its application to the cuprous oxides*, Rev. Mod. Phys. **63**, 1 (1991).

[6] J. D. Reger and A. P. Young, *Monte Carlo simulations of the spin-1/2 Heisenberg antiferromagnet on a square lattice*, Phys. Rev. B **37**, 5978 (1988).

[7] S. Chakravarty, B. I. Halperin, and D. R. Nelson, *Low-temperature behavior of two-dimensional quantum antiferromagnets*, Phys. Rev. Lett. **60**, 1057 (1988); *Two-dimensional quantum Heisenberg antiferromagnet at low temperatures*, Phys. Rev. B **39**, 2344 (1989).

[8] P. Hasenfratz and F. Niedermayer, *Finite size and temperature effects in the AF Heisenberg model*, Z. Phys. B **92**, 91 (1993).

[9] U.-J. Wiese and H.-P. Ying, *A determination of the low energy parameters of the 2-d Heisenberg antiferromagnet*, Z. Phys. B **93**, 147 (1994).

[10] A. V. Chubukov, S. Sachdev, and J. Ye, *Theory of two-dimensional quantum Heisenberg antiferromagnets with a nearly critical ground state*, Phys. Rev. B **49**, 11919 (1994).

[11] S. Sachdev, *Quantum Phase Transitions*, Cambridge University Press, 2001.

[12] S. Sachdev, *Quantum criticality: Competing ground states in low dimensions*, Science **288**, 475 (2000).

[13] M. A. Kastner, R. J. Birgeneau, G. Shirane, and Y. Endoh, *Magnetic, transport, and optical properties of monolayer copper oxides*, Rev. Mod. Phys. **70**, 897 (1998).

[14] G. Xiao, M. Z. Cieplak, A. Gavrin, F. H. Streitz, A. Bakhshai, and C. L. Chien, *High-temperature superconductivity in tetragonal perovskite structures: Is oxygen-vacancy order important?*, Phys. Rev. Lett. **60**, 1446 (1988).

[15] S.-W. Cheong, A. S. Cooper, L. W. Rupp, Jr., B. Batlogg, J. D. Thompson, and Z. Fisk, *Magnetic dilution study in La_2CuO_4: Comparison with other two-dimensional magnets*, Phys. Rev. B **44**, 9739 (1991); S. T. Ting, P. Pernambuco-Wise, J. E. Crow, E. Manousakis, and J. Weaver, *Magnetic properties of $La_2Cu_{1-x}M_xO_4$ with M=Zn and Ni*, *ibid.* **46**, 11772 (1992); M. Corti, A. Rigamonti, F. Tabak, P. Carretta, F. Licci, and L. Raffo, *^{139}La NQR relaxation and μSR study of Zn-doping effects in La_2CuO_4*, *ibid.* **52**, 4226 (1995); P. Carretta, A. Rigamonti, and R. Sala, *Spin dynamics in a two-dimensional disordered $S = 1/2$ Heisenberg paramagnet from ^{63}Cu NQR relaxation in Zn-doped La_2CuO_4*, *ibid.* **55**, 3734 (1997).

[16] O. P. Vajk, P. K. Mang, M. Greven, P. M. Gehring, and J. W. Lynn, *Quantum impurities in the two-dimensional spin one-half Heisenberg antiferromagnet*, Science **295**, 1691 (2002).

[17] A. V. Mahajan, H. Alloul, G. Collin and J. F. Marucco, *^{89}Y NMR probe of Zn induced local moments in $YBa_2(Cu_{1-y}Zn_y)_3O_{6+x}$*, Phys. Rev. Lett. **72**, 3100 (1994).

[18] J. Bobroff, H. Alloul, Y. Yoshinari, A. Keren, P. Mendels, N. Blanchard, G. Collin, and J.-F. Marucco, *Using Ni substitution and ^{17}O NMR to probe the susceptibility $\chi'(q)$ in cuprates* , Phys. Rev. Lett. **79**, 2117 (1997).

[19] M.-H. Julien, T. Fehér, M. Horvati, C. Berthier, O. N. Bakharev, P. Ségransan, G. Collin, and J.-F. Marucco, *^{63}Cu NMR evidence for enhanced antiferromagnetic correlations around Zn impurities in $YBa_2Cu_3\ O_{6.7}$*, Phys. Rev. Lett. **84**, 3422 (2000).

[20] M. Takigawa, N. Motoyama, H. Eisaki, and S. Uchida, *Field-induced staggered magnetization near impurities in the $S = 1/2$ one-dimensional Heisenberg antiferromagnet Sr_2CuO_3*, Phys. Rev. B **55**, 14129 (1997).

[21] N. Nagaosa and T.-K. Ng, *Nonmagnetic impurity in the spin-gap state*, Phys. Rev. B **51**, 15588 (1995).

[22] A. W. Sandvik, E. Dagotto, and D. J. Scalapino, *Nonmagnetic impurities in spin-gapped and gapless Heisenberg antiferromagnets*, Phys. Rev. B **56**, 11701 (1997).

[23] G. B. Martins, M. Laukamp, J. Riera, and E. Dagotto, *Local enhancement of antiferromagnetic correlations by nonmagnetic impurities*, Phys. Rev. Lett. **78**, 3563 (1997); M. Laukamp *et al.*, *Enhancement of antiferromagnetic correlations induced by nonmagnetic impurities: Origin and predictions for NMR experiments*, Phys. Rev. B **57**, 10755 (1998).

[24] S. Sachdev, C. Buragohain, and M. Vojta, *Quantum impurity in a nearly critical two-dimensional antiferromagnet*, Science **286**, 2479 (1999); M. Vojta, C. Buragohain, and S. Sachdev, *Quantum impurity dynamics in two-dimensional antiferromagnets and superconductors*, Phys. Rev. B **61**, 15152 (2000).

[25] N. Bulut, D. Hone, D. J. Scalapino, and E. Y. Loh, *Static vacancies on a 2D Heisenberg spin-1/2 antiferromagnet*, Phys. Rev. Lett. **62**, 2192 (1989).

[26] N. Nagaosa, Y. Hatsugai, and M. Imada, *Spin wave theory of the two-dimensional Heisenberg antiferromagnet coupled with localized holes*, J. Phys. Soc. Jpn. **58**, 978 (1989).

[27] P. Schlottmann, *Perturbative approximation scheme for isolated impurity bonds in the two-dimensional spin-1/2 Heisenberg antiferromagnet*, J. Appl. Phys. **75**, 5532 (1994).

[28] V. N. Kotov, J. Oitmaa, and O. Sushkov, *Magnetic impurity in the two-dimensional Heisenberg antiferromagnet*, Phys. Rev. B **58**, 8495 (1998); *Local magnetic impurities in the two-dimensional quantum Heisenberg antiferromagnet*, *ibid.* **58**, 8500 (1998).

[29] O. P. Sushkov, *Spin-1/2 magnetic impurity in a two-dimensional magnetic system close to a quantum critical point*, Phys. Rev. B **62**, 12135 (2000).

[30] K. Murayama and J. Igarashi, *A multiple scattering theory for a magnetic impurity coupled to quantum antiferromagnets in quasi-two dimensions*, J. Phys. Soc. Jpn. **66**, 1157 (1996).

[31] S. Sachdev and M. Vojta, *Quantum impurity in an antiferromagnet: Nonlinear sigma model theory*, Phys. Rev. B **68**, 064419 (2003).

[32] O. P. Sushkov, *Long-range dynamics related to magnetic impurities in the two-dimensional Heisenberg antiferromagnet*, Phys. Rev. B **68**, 094426 (2003).

[33] A. V. Syromyatnikov and S. V. Maleyev, *Frustrated two-level impurities in two-dimensional antiferromagnets*, Phys. Rev. B **72**, 174419 (2005); *Frustrated impurity spins in ordered two-dimensional quantum antiferromagnets*, Phys. Rev. B **74**, 184433 (2006).

[34] F. Anfuso and S. Eggert, *Knight shifts around vacancies in the 2D Heisenberg model*, Phys. Rev. Lett. **96**, 017204 (2006).

[35] S. Eggert, O. F. Syljuåsen, F. Anfuso, and M. Andres, *Universal alternating order around impurities in antiferromagnets*, Phys. Rev. Lett. **99**, 097204 (2007).

[36] A. L. Chernyshev, Y. C. Chen, and A. H. Castro Neto, *Diluted quantum antiferromagnets: Spin excitations and long-range order*, Phys. Rev. B **65**, 104407 (2002).

[37] L. Wang and A. W. Sandvik, *Low-energy dynamics of the two-dimensional $S = 1/2$ Heisenberg antiferromagnet on percolating clusters*, Phys. Rev. Lett. **97**, 117204 (2006), and references therein.

[38] S. Eggert and I. Affleck, *Impurities in $S = 1/2$ Heisenberg antiferromagnetic chains: Consequences for neutron scattering and Knight shift*, Phys. Rev. Lett. **75**, 934 (1995).

[39] S. Eggert and S. Rommer, *Universal crossover behavior of a magnetic impurity and consequences for doping in spin-1/2 Chains*, Phys. Rev. Lett. **81**, 1690 (1998); S. Rommer and S. Eggert, *Impurity corrections to the thermodynamics in spin chains using a transfer-matrix DMRG method*, Phys. Rev. B **59**, 6301 (1999).

[40] S. Fujimoto and S. Eggert, *Boundary susceptibility in the spin-1/2 chain: Curie-like behavior without magnetic impurities*, Phys. Rev. Lett. **92**, 037206 (2004).

[41] J. Sirker, N. Laflorencie, S. Fujimoto, S. Eggert, and I. Affleck, *Chain breaks and the susceptibility of $Sr_2Cu_{1-x}Pd_xO_{3+\delta}$ and other doped quasi-one-dimensional antiferromagnets*, Phys. Rev. Lett. **98**, 137205 (2007); J. Sirker, S. Fujimoto, N. Laflorencie, S. Eggert, and I. Affleck, *Thermodynamics of impurities in the anisotropic Heisenberg spin-1/2* chain, J. Stat. Mech., P02015 (2008).

[42] E. H. Lieb and D. C. Mattis, *Ordering energy levels of interacting spin systems*, J. Math. Phys. (N.Y.) **3**, 749 (1962).

[43] M. Troyer, *Static and dynamic holes in a quantum critical antiferromagnet*, Prog. Theor. Phys. Supp. **145**, 326 (2002).

[44] A. B. Harris and S. Kirkpatrick, *Low-frequency response functions of random magnetic systems*, Phys. Rev. B **16**, 542 (1977).

[45] A. Aharony, R. J. Birgeneau, A. Coniglio, M. A. Kastner, and H. E. Stanley, *Magnetic phase diagram and magnetic pairing in doped* La_2CuO_4, Phys. Rev. Lett. **60**, 1330 (1988).

[46] K. Hida, *Low temperature properties of the double layer quantum Heisenberg antiferromagnet—modified spin wave method—*, J. Phys. Soc. Jpn. **59**, 2230 (1990).

[47] A. J. Millis and H. Monien, *Spin gaps and spin dynamics in* $La_{2-x}Sr_xCuO_4$ *and* $YBa_2Cu_3O_{7-\delta}$, Phys. Rev. Lett. **70**, 2810 (1993); *Spin gaps and bilayer coupling in* $YBa_2Cu_3O_{7-\delta}$ *and* $YBa_2Cu_4O_8$, Phys. Rev. B **50**, 16606 (1994).

[48] A. W. Sandvik and D. J. Scalapino, *Order-disorder transition in a two-layer quantum antiferromagnet*, Phys. Rev. Lett. **72**, 2777 (1994).

[49] A. W. Sandvik, A. V. Chubukov, and S. Sachdev, *Quantum critical behavior in a two-layer antiferromagnet*, Phys. Rev. B **51**, 16483 (1995).

[50] A. V. Chubukov and D. K. Morr, *Phase transition, longitudinal spin fluctuations, and scaling in a two-layer antiferromagnet*, Phys. Rev. B **52**, 3521 (1995).

[51] Y. Matsushita, M. P. Gelfand, and C. Ishii, *Phase transitions in bilayer Heisenberg model with general couplings*, J. Phys. Soc. Jpn. **66**, 3648 (1997).

[52] V. N. Kotov, O. Sushkov, Z. Weihong, and J. Oitmaa, *Novel approach to description of spin-liquid phases in low-dimensional quantum antiferromagnets*, Phys. Rev. Lett. **80**, 5790 (1998).

[53] N. Elstner and R. R. P. Singh, *Strong-coupling expansions at finite temperatures: Application to quantum disordered and quantum critical phases*, Phys. Rev. B **57**, 7740 (1998).

[54] P. V. Shevchenko, A. W. Sandvik, and O. P. Sushkov, *Double-layer Heisenberg antiferromagnet at finite temperature: Brueckner theory and quantum Monte Carlo simulations*, Phys. Rev. B **61**, 3475 (2000).

[55] S. Sachdev, M. Troyer, and M. Vojta, *Spin orthogonality catastrophe in two-dimensional antiferromagnets and superconductors*, Phys. Rev. Lett. **86**, 2617 (2001).

[56] L. Wang, K. S. D. Beach, and A. W. Sandvik, *High-precision finite-size scaling analysis of the quantum-critical point of S=1/2 Heisenberg antiferromagnetic bilayers*, Phys. Rev. B **73**, 014431 (2006).

[57] W. Brenig, *Finite-temperature properties of the two-dimensional SU(2) Kondo necklace*, Phys. Rev. B **73**, 104450 (2006).

[58] W. Brenig, *Magnetism in the disordered two-dimensional Kondo-necklace*, Int. J. Mod. Phys. B **21**, 2245 (2007).

[59] H. G. Evertz, *The loop algorithm*, Adv. Phys. **52**, 1 (2003).

[60] S. Sachdev, private communication.

[61] K. H. Höglund and A. W. Sandvik, unpublished.

[62] A. Lüscher and O. P. Sushkov, *Long-range dynamics of magnetic impurities coupled to a two-dimensional Heisenberg antiferromagnet* , Phys. Rev. B **71**, 064414 (2005).

[63] M. A. Metlitski and S. Sachdev, *Impurity spin textures across conventional and deconfined quantum critical points of two-dimensional antiferromagnets*, Phys. Rev. B **76**, 064423 (2007).

[64] F. Milla and T. M. Rice, *Analysis of magnetic resonance experiments in $YBa_2Cu_3O_7$*, Physica C **157**, 561 (1989); A. J. Millis, H. Monien, and D. Pines, *Phenomenological model of nuclear relaxation in the normal state of $YBa_2Cu_3O_7$*, Phys. Rev. B **42**,167 (1990); A. W. Sandvik and D. J. Scalapino, *Spin dynamics of La_2CuO_4 and the two-dimensional Heisenberg model*, Phys. Rev. B **51**, 9403 (1995).

[65] W. Guo and A. W. Sandvik, work in progress.

[66] M. A. Metlitski and S. Sachdev, *Edge and impurity response in two-dimensional quantum antiferromagnets*, Phys. Rev. B **78**, 174410 (2008).

[67] S. Wenzel, Ph. D. Thesis, University of Leipzig, 2008; R. G. Melko, private communication.

Svensk resumé

Många av de intressantaste fenomenen inom dagens materialfysik uppstår ur det intrikata samspelet mellan ett stort antal elektroner. Det mest berömda exemplet är högtemperatursupraledare. Varken klassiska teorier eller modeller där elektronerna är oberoende av varandra kan förklara fenomenen. Istället döljer sig förklaringen till de häpnadsväckande makroskopiska effekterna i det kollektiva elektronbeteende som just laddningarnas starka ömsesidiga växelverkan leder till.

I vissa kopparoxider, till exempel La_2CuO_4, är det känt att valenselektronerna till följd av en stark ömsesidig växelverkan lokaliseras en och en till kopparatomerna i föreningens CuO_2 plan. Elektronernas inneboende magnetiska moment—spinnet—får då en avgörande roll för systemets elektroniska och magnetiska egenskaper. Om föreningarna dopas med extra laddningsbärare kan de bli supraledande. Men exakt hur det går till är oklart—en enkel mikroskopisk förklaring saknas.

De teoretiska modellerna för starkt korrelerade elektronsystem är för det mesta ytterst invecklade matematiskt sett och de kan inte lösas exakt. Därför har bland annat supraledning vid höga temperaturer inte kunnat hittills härledas ur någon given matematisk modell som till exempel favoritkandidaten Hubbard modellen. Däremot är det känt att den nära besläktade Heisenberg modellen beskriver de odopade kopparoxidernas elektromagnetiska egenskaper mycket bra. Det är den enklaste modellen för mikroskopisk magnetism i allmänhet—den beskriver hur lokaliserade spinn effektivt växelverkar.

Många av Heisenberg modellens egenskaper är väl kartlagda. Den

har undersökts i otaliga studier som på senare tider ofta motiverats med just kopplingen till högtemperatursupraledarna. Modellen är också en användbar och populär utgångspunkt för studier av de fundamentala aspekterna hos starkt korrelerade spinnsystem. Trots ansträngningarna har ingen exakt lösning funnits. De analytiska utredningarna bygger för det mesta på antaganden och förenklingar vars inverkningar på slutresultatet ofta är oklara. Numeriska studier i sin tur kan i vissa fall behandla modellen exakt, men närmevärdesresultaten är alltid för ett system av given storlek och de måste extrapoleras till det makroskopiska. Oftast behövs bägge tillvägagångssätten. En relevant fråga som inte utretts i detalj är vad effekterna av orenheter är i Heisenberg modellen.

Min avhandling undersöker inverkan av olika defekter som till exempel enskilda vakanser och öppna kanter på Heisenberg modellens magnetiska egenskaper. En beprövat effektiv numerisk metod har använts—en kvantmekanisk Monte Carlo teknik—för att utföra omfattande datorsimuleringar på två dedikerade Linux datorkluster som byggts för ändamålet. Arbetet hör till området beräkningsfysik. En central strategi har varit att numeriskt pröva om vissa analytiska förutsägelser gällande modellen håller sträck.

För en spinn-S orenhet kopplad till en magnetiskt ordnad Heisenberg modell hade en magnetisk respons om $S^2/3T$ förutspåtts vid låga temperaturer. Våra numeriska resultat bekräftade detta men påvisade också att det finns ytterligare ett bidrag—en med temperaturen logaritmiskt divergerande trend—som teorin inte förutsett. I den så kallade kvantkritiska fasen kunde vi på basen av mycket noggranna numeriska data avgöra att responsen i det fallet är besynnerlig, som om orenheten effektivt hade spinn olika S. I samarbete med analytiska ansträngningar kunde vi utröna att den av orenheten inducerade magnetiseringen fördelas över hela det kritiska värdsystemet. Slutligen undersöktes inverkan av öppna kanter på Heisenberg modellens magnetiska suskeptibilitet. Något överraskande visade resultaten att spinnen nära kanterna uppvisar en minskad respons på grund av förändringar i korrelationerna mellan de närmaste grannarna.

ISBN 978-952-12-2415-7

UNIPRINT
Åbo 2010